Antarctic Science 26(3), 267–275 (2014) © Antarctic Science Ltd 2013 doi:10.1017/S0954102013000758

Unusual signals recorded by ocean bottom seismometers in the flooded caldera of Deception Island volcano: volcanic gases or biological activity?

DANIEL C. BOWMAN[1,2] and WILLIAM S.D. WILCOCK[3]

[1]*GZA GeoEnvironmental, 249 Vanderbilt Avenue, Norwood, MA 02062, USA*
[2]*Department of Geological Sciences, Box 3315, University of North Carolina, Chapel Hill, NC 27599, USA*
[3]*School of Oceanography, Box 357940, University of Washington, Seattle, WA 98195, USA*
daniel.bowman@unc.edu

Abstract: An ocean bottom seismometer (OBS) network was deployed for 1 month at Deception Island volcano, Antarctica, in early 2005. Although only two volcano-tectonic and three long-period events were observed, the three OBSs located > 2 km apart inside the caldera detected over 3900 events that could not be attributed to known volcanic or hydrothermal sources. These events are found on one instrument at a time and occur in three types. Type 1 events resemble impulsive signals from biological organisms while type 2 and type 3 events resemble long-period seismicity. The largest number of events was observed in a region of volcanic resurgence and hydrothermal venting. All three types occur together suggesting a common cause and they show evidence for a diurnal distribution. The events are most likely to be due to aquatic animals striking the sensors, but a geological source is also possible. In the first case, these signals indicate the presence of a biological community confined to the caldera. In the second case, they imply widespread hydrothermal activity in Port Foster. Future OBS experiments should bury the seismometers, include a hydrophone, deploy instruments side-by-side, or include a video camera to distinguish between biological and geological events.

Received 27 October 2012, accepted 24 September 2013, first published online 26 November 2013

Key words: biological signal, degassing, hydrothermal activity, undersea seismic network, volcanic seismology

Introduction

Active volcanoes generate a wide variety of signals related to tectonic deformation, magma movement, hydrothermal circulation and slope instabilities (e.g. Gasparini *et al*. 1992). Earthquake monitoring represents an important tool for understanding volcanic processes and forecasting eruptions. Volcanic seismicity typically takes three forms: volcano-tectonic (VT), long-period (LP) and tremor. Volcano-tectonic events have a broadband spectral signature and are generated by brittle failure from stresses inside the volcano, thus resembling tectonic earthquakes. Whereas, LP events and tremor tend to have maximum energy between approximately 0.5–5 Hz and are created by volcanic fluids. Since both VT and LP events are proxies of volcanic unrest, quantifying their spatial and temporal occurrence patterns is critical in volcano monitoring (Chouet 1996). Although most volcanism occurs in submarine regimes, long-term seismic monitoring is almost exclusively limited to subaerial settings because these volcanoes generally represent a larger hazard and land-based seismic networks can be installed and operated more easily. It is quite possible that the full range of volcanic signals in submarine settings has not yet been documented.

Deception Island is a stratovolcano in the South Shetland Islands, an archipelago that lies between the southern tip of South America and the Antarctic Peninsula. The subaerial portion of the volcano consists of a glaciated, horseshoe-shaped island opening to the south-east (Fig. 1). The outer coast of the island consists of cliffs and the inner coast is made up of sand and gravel beaches (Smellie 2001). The flooded central portion of the volcano is called Port Foster. It is roughly circular and ranges from 5–9 km in diameter. The floor of Port Foster consists of a flat basin lying 160 m below sea level. The basin is ringed by a shallow shelf extending approximately 1 km from the inner shoreline of the island (Barclay *et al*. 2009).

Deception Island is located in a backarc spreading basin that is likely to be related to subduction rollback at the South Shetland trench (Barker & Austin 1998). The volcanic edifice consists of tuffs, lava and phreatomagmatic deposits. It is difficult to ascertain the age of Deception Island, but the subaerial portion of the volcano is likely to be < 100 000 years old (Smellie 2001). Port Foster is generally thought to be a volcanic caldera (Smellie 2001), although some have suggested that it is a tectonic depression (Rey *et al*. 1995). The floor of Port Foster consists of a layer of unconsolidated sediment approximately 1.2 km thick underlain by denser material (Ben-Zvi *et al*. 2009).

There have been six eruptions at Deception Island in historic time, all of which have produced little magma and lasted from hours to days. Hot springs and fumaroles can be

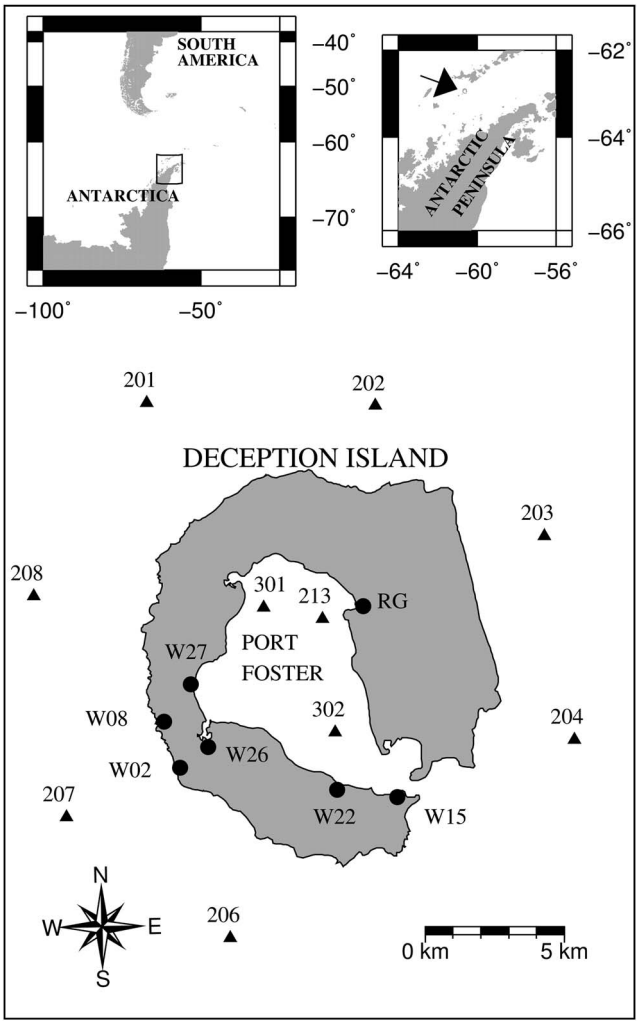

Fig. 1. Map of Deception Island volcano and the seismic monitoring network deployed in January and February 2005. Land seismic stations are shown by labelled black circles and ocean bottom seismometers by labelled black triangles. The inset maps show regional location of Deception Island near the Antarctic Peninsula.

found in several places on the island (Ibáñez *et al*. 2000), and a recent study found evidence for a magma chamber < 2 km below the floor of Port Foster (Ben-Zvi *et al*. 2009, Zandomeneghi *et al*. 2009). One area of Port Foster may be rising up to 0.3 m year^{-1} due to a shallow magmatic intrusion (Cooper *et al*. 1998). Seawater in parts of Port Foster is 2°C warmer than elsewhere in the bay, and gas geothermometry indicates that shallow aquifers on the volcano can reach temperatures of up to 219°C (Ortiz *et al*. 1992).

Seismic monitoring has occurred regularly on Deception Island since the 1950s with the exception of a 16-year gap beginning in 1970 when an eruption destroyed the monitoring station. Seismographs maintained by the Argentinean and Spanish governments, as well as temporary field deployments, have recorded seismic activity every summer since 1986 (Ibáñez *et al*. 2003a). This activity has ranged from a thousand earthquakes a month in the late 1980s (Vila *et al*. 1992) to eight earthquakes per month in December 1998 (Ibáñez *et al*. 2003b). However, LP events numbered up to 150 per day during the 1998–99 field season. Seismic swarms also occur on Deception Island, notably in early 1999, when up to 80 earthquakes per day were recorded (Ibáñez *et al*. 2003b). Signals recorded at Deception Island often originate proximal to the sensor, with instruments several kilometres away remaining quiet (Ibáñez *et al*. 2003b). Ibáñez *et al*. (2003a) describes an implementation of a zero lag cross correlation technique modified for circular wave front geometry that located LP events several hundred metres from a seismic array near Port Foster. At Deception Island such events originate from shallow hydrothermal activity (Ibáñez *et al*. 2000, Ibáñez *et al*. 2003a).

In this paper we present results from the deployment of three-component seismometers in the flooded caldera and flanks of Deception Island volcano, South Shetland Islands, Antarctica. We quantify the seismic activity of the volcano during the 2005 field season and place it in the context of past seismic studies at Deception Island. We also describe thousands of signals of unknown origin. We suggest possible sources for these signals as well as describe improvements to instrumentation and deployment methods that will allow future networks to determine their cause.

Instruments and methods

In the 2004–05 summer an extensive network of land seismometers and OBSs was deployed at Deception Island volcano as part of an active source tomography experiment (Ben-Zvi *et al*. 2009, Zandomeneghi *et al*. 2009). The OBSs were released at the surface and sank through the water column, activating after reaching the ocean floor. Following seven days of airgun shooting, a subset of the seismic instruments was left in place for around a month to monitor seismicity. This earthquake monitoring network (Fig. 1) comprised seven land stations around the shores of Port Foster and ten OBSs, seven on the outer flanks of the volcano and three in Port Foster. The OBSs on the flanks were deployed at depths ranging from 119 m to 475 m. The three OBSs inside Port Foster, stations 213, 301 and 302, were deployed at depths of 143 m, 170 m and 125 m, respectively. Each OBS was continuously recording with a sampling rate of 125 Hz and was equipped with a broadband self-levelling three-component seismometer and a differential pressure gauge designed to record LP acoustic signals.

Seismic events were detected using the 'dbdetect' function in the Datascope seismic database system (Lindquist & Quinlan 2009). We searched for signals in two bands: 1–5 Hz for local events and 0.3–1 Hz for regional events. The detection algorithm flagged a 0.25-second window if it

https://doi.org/10.1017/S0954102013000758 Published online by Cambridge University Press

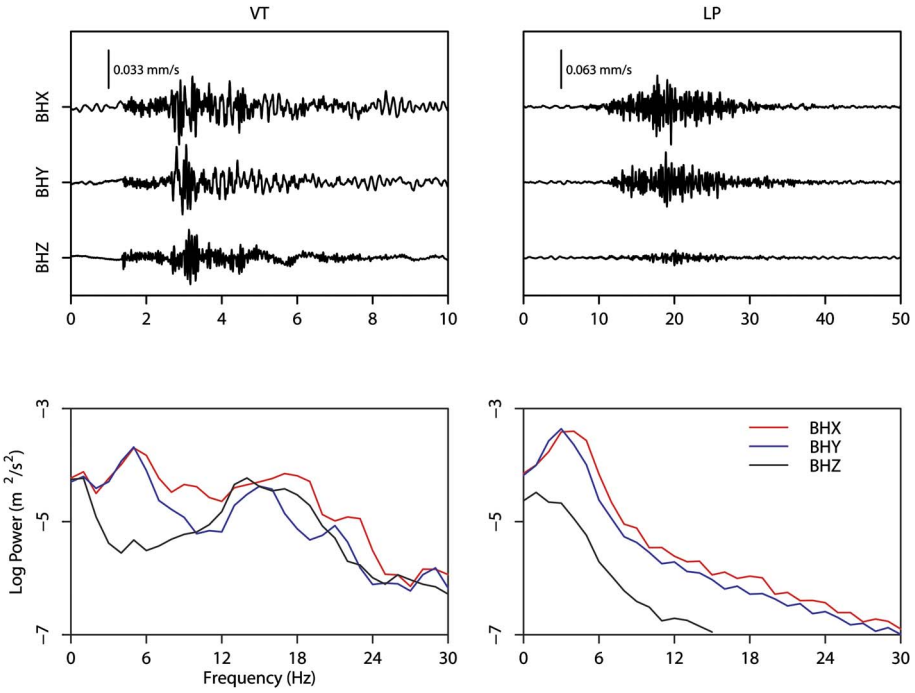

Fig. 2. Seismograms and power spectra for a volcano-tectonic (VT) and a long-period (LP) event recorded on station 302. Note the difference in timescales. A 0.5 Hz high pass filter was applied to remove low frequency background noise.

had five times the root mean square amplitude of the previous 200 seconds. These detections were then visually examined to eliminate airgun shots and whale calls, and to identify earthquakes. We classified an event as VT if it was reported on more than one station, had a broadband spectral signature and was located within the seismic network. We classified an event as LP if it was detected by more than one station, had a low frequency spectral signature and was located in the seismic network.

A detection algorithm was also developed in MATLAB to find signals seen on individual OBSs in Port Foster. This programme captured 4-second long windows of seismogram data. If the average absolute value of the amplitude in a time window was at least three times as large as the average absolute value of the amplitude in the surrounding 100 seconds of data, the window was marked as a potential event. The window size was chosen based on the observed duration of the high amplitude portion of Port Foster events. In addition, these parameters produced the lowest number of false positives. After running the detection algorithm, Port Foster event candidates were then visually examined and categorized based on signal characteristics.

We examined the distribution of these events by time of day and applied a binomial test to determine if the level of activity varied significantly with the diurnal cycle. The binomial test is a statistical method to determine the

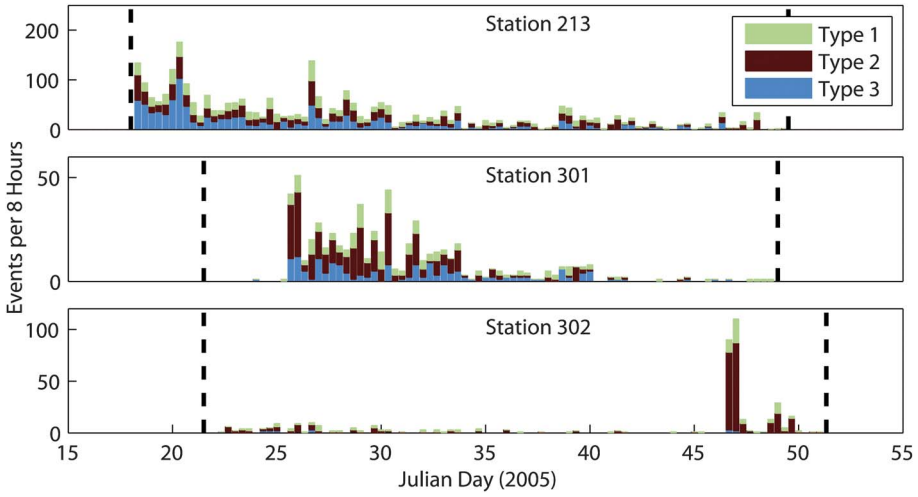

Fig. 3. Histogram of events recorded in 8-hour intervals at each of the three OBSs inside Port Foster, colour coded by event type. Dashed vertical lines indicate when the instruments were recording.

https://doi.org/10.1017/S0954102013000758 Published online by Cambridge University Press

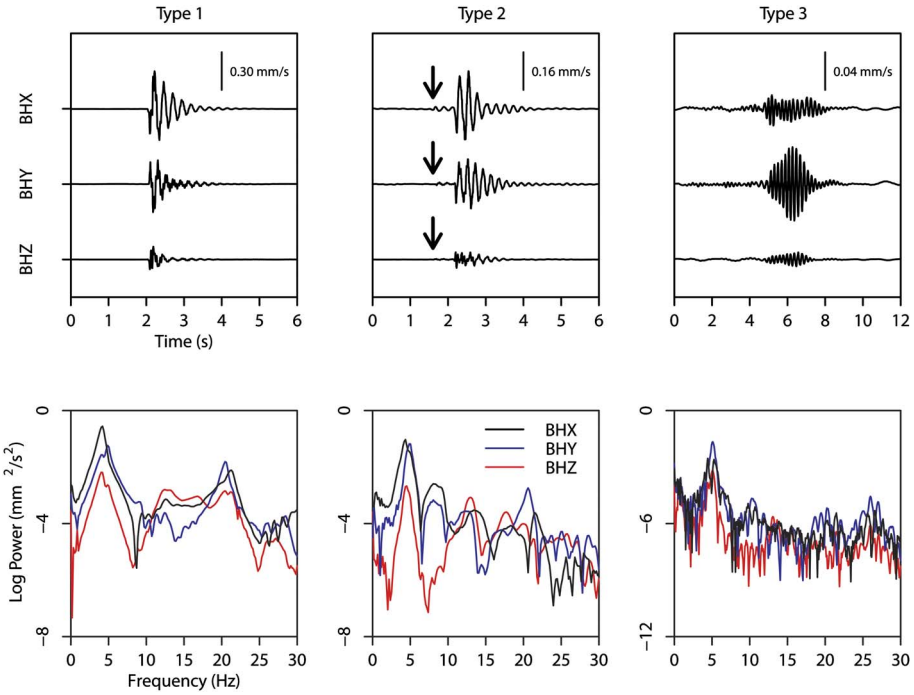

Fig. 4. Seismograms and corresponding spectra for type 1, type 2 and type 3 events recorded on station 302. The arrow on the type 2 seismogram indicates the low amplitude initial arrival that distinguishes this category from type 1 events. Note the different timescale for the type 3 seismogram.

likelihood that an observed distribution of independent events is a result of random chance or a biased system (Sterne 1954). We ran a second series of binomial tests after applying a simple declustering algorithm that eliminated all but the first event in each hour irrespective of event type to account for the clustering in our data. We calculated several autocorrelations of Port Foster event occurrences per hour using the 'stats' package for the R programming language (R Core Team 2012). The autocorrelation shifted the time series 1 hour at a time, up to a 120-hour lag.

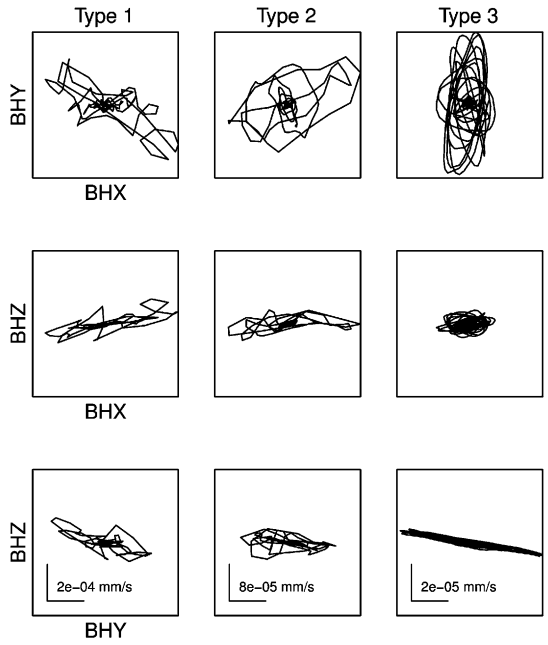

Fig. 5. Particle motions for the events shown in Fig. 4. Most motion occurs in the XY plane.

Volcanic seismicity at Deception Island during the 2005 field season

Two VT and three LP events were recorded at Deception Island during the study period, and no tremor was identified. Both VT events were only recorded on the OBSs inside Port Foster (Fig. 2). The three LP events had dominant frequencies at and below 5 Hz (Fig. 2). Two of the three occurred less than an hour apart.

The three OBSs located on the floor of Port Foster collectively recorded over 3900 other events during the study period. These Port Foster events often have good signal-to-noise ratios but each event is only recorded on one of the three stations in Port Foster. Similar signals were not observed on OBSs on the volcano flanks or on land stations. The events typically last 1–10 seconds and their rates of occurrence vary from 0 to almost 60 per hour (Fig. 3). Activity decreased over the month long study period but the patterns are not consistent by station. Station 213 recorded the most activity with 2914 events and the highest levels of activity early in the deployment, station 301 recorded 616 events, and station 302 recorded only 407 events with most of them near the end of the deployment. These events have a dominant frequency between 4–6 Hz and the particle motions are primarily in the horizontal plane with no preferred orientation.

https://doi.org/10.1017/S0954102013000758 Published online by Cambridge University Press

Table I. Port Foster event distribution by time of day[1].

Station	Depth (m)	Event type	Day events	Night events	Total	Night fraction	Night probability
213	143	All	2050	864	2914	0.30	0.72
301	170	All	470	146	616	0.24	0.0014
302	125	All	372	35	407	0.09	<0.0001
All	–	Type 1	804	210	1014	0.21	<0.0001
All	–	Type 2	1187	394	1581	0.25	<0.0001
All	–	Type 3	901	441	1342	0.33	>0.99
All	–	All	2892	1045	3937	0.27	0.00013
213	143	Declustered	369	157	526	0.30	0.65
301	170	Declustered	173	58	231	0.25	0.098
302	125	Declustered	100	18	118	0.15	0.00033
All	–	Declustered	642	233	875	0.27	0.052

[1] Events are partitioned into day and night based on a seasonal approximation of 7 hours of night (0100 to 0800 GMT) and 17 hours of daylight. For a random population a fraction of 0.29 of the events would be expected at night. Probability of night is the binomial probability that the number of night events would be less than observed, assuming a random distribution. The events are declustered where noted by eliminating all but the first event on each ocean bottom seismometer (OBS) in each hour irrespective of type.

We observed three types of Port Foster events (Fig. 4): a short, impulsive waveform (type 1), a low amplitude arrival followed by a higher amplitude arrival (type 2) and an emergent wave train with one or more high amplitude pulses (type 3).

Type 1 events are impulsive and typically last 1–2 seconds. The signal decays rapidly and smoothly from its peak amplitude. No separate arrivals are apparent in seismograms (Fig. 4) or particle motions (Fig. 5). Type 1 contain a broadband component to 30 Hz in addition to the frequency peak between 4–6 Hz. They are the least common type of event, with 1014 recorded during the study period.

Type 2 events have a low amplitude initial arrival followed by a much higher amplitude second arrival (Fig. 4). These arrivals are usually separated by less than a second, with the entire signal lasting 2–4 seconds. The particle motions (Fig. 5) and spectral content for the two arrivals are similar to type 1 events. The first motions of the two arrivals on the vertical channel have reversed polarity around half the time. Type 2 events are the most common, with 1581 recorded during the study period.

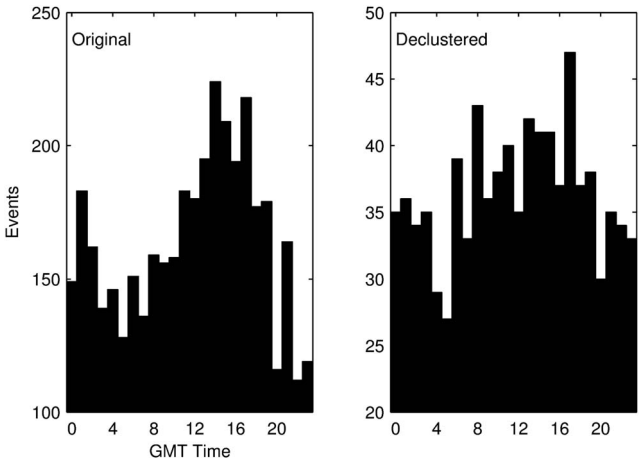

Fig. 6. a. Histogram showing the distribution of all Port Foster events by hour of day. **b.** Histogram showing the distribution of declustered Port Foster events by hour of day (declustering removed all but the first event in each hour on each instrument).

Type 3 events have a more gradual onset and may last up to 10 seconds. Type 3 signals are more complex than the other two types and can consist of multiple arrivals (Fig. 4). Horizontal motions can vary from a simple oval track to multiple tracks in different orientations (Fig. 5). The spectral content of type 3 events mainly lies in the 4–6 Hz band, and the broadband component is relatively less energetic than the other two types. Some type 3 events also have a dominant frequency that smoothly increases or decreases for the duration of the signal. There were 1342 type 3 events recorded during the study period.

The binomial tests for diurnal dependence found statistically significant deviations from the expected distribution of Port Foster events. For example, the binomial test predicts that 38% of the observed events should fall between 0900 and 1800 GMT, but we found that 48% of the events occurred during that time (Fig. 6a).

Events occur significantly less often at night than expected at a 95% confidence level for the full event list, type 1 events and type 2 events but not for type 3 events (Table I). In fact, type 3 events have a significant increase in activity at night. Stations 301 and 302 showed a significant decrease in events at night but station 213 did not have a significant change in event rate.

The hour by hour distribution of the declustered catalogue (Fig. 6b) shows the same general pattern as for the full dataset but it is more muted. A binomial test shows that the rate of declustered night-time events is not significantly lower at the 95% confidence level (Table I). When stations are analysed individually the decrease is only significant on station 302.

https://doi.org/10.1017/S0954102013000758 Published online by Cambridge University Press

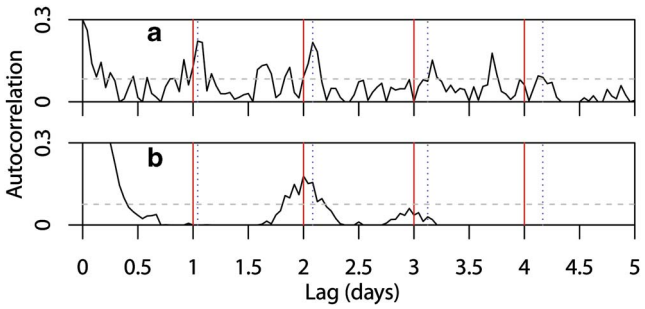

Fig. 7. a. Correlogram of Port Foster events per hour at station 302 from Julian day 22 through 45. **b.** Correlogram of Port Foster events per hour at station 302 from Julian day 22 through 50, including two large clusters between Julian day 45 and 50. Solid vertical line indicates 24-hour (diurnal) periodicity, dashed vertical line indicates 25-hour (tidal) periodicity. Dashed horizontal line indicates the 95% confidence limit (R Core Team, 2012).

To further investigate the periodicity of the data, we also performed an autocorrelation on the number of events per hour. We tested the combined dataset as well as each station and event type individually. There was no evidence of a significant diurnal or tidal periodicity, except on the total number of events per hour on station 302 from Julian day 22–45 when large clusters were absent. This autocorrelation (Fig. 7a) shows a periodicity of around 25 hours, which is significant at the 95% confidence level. There is one significant peak centred at 48 hours on station 302 if the large clusters of events between Julian day 45 and 50 are included (Fig. 7b).

Discussion

At a regional scale, Deception Island was seismically quiet during the study, which is consistent with previous seismic surveys at the volcano that show that the seismicity is episodic (Ibáñez *et al*. 2003a). The large number of events recorded at single stations in Port Foster indicates that high levels of localized activity were present inside the flooded caldera of the volcano.

Transient signals recorded on single OBSs in shallow water are often attributed to biological activity, and such activity is known to correlate with the day/night cycle (Buskirk *et al*. 1981). Thus, we performed several statistical tests to determine if the events were sensitive to the time of day. However, some caution must be exercised in interpreting these results. Studies of tidal triggering on volcanoes have established that only a small number of non-random events are required to produce a strong apparent temporal correlation (e.g. Rydelek *et al*. 1992). The binomial test assumes each event is independent while the histograms of their occurrence throughout the experiment (Fig. 3) show that they are strongly clustered in time. For example, on station 302 around half the events occur during one 16-hour interval, this might be sufficient in itself to generate the observed diurnal distribution. The declustering algorithm was designed to reduce this effect, but it may also attenuate a true diurnal signal especially for stations 301 and 213. This is because these stations often had at least one event per hour irrespective of the time of day. With this in mind, we propose three possible causes for these events: instrument settling, biological organisms striking the sensor and geological activity.

Rather than being anchored to the sea floor, the OBSs were released at the surface and allowed to drift down. If the substrate was soft and unconsolidated, the instruments may have been poorly coupled to the sea floor. This could explain the strongly horizontal particle motions of the Port Foster events (Duennebier & Sutton 2007). The localized events we see could also be due to the instrument settling into the soft sea floor after impact. However, it is difficult to understand how instrument settling would produce the three distinct types of event we observe. We would also expect a much higher number of events at the beginning of the deployment relative to the middle and end. Although there is a decrease in the number of events per hour at stations 213 and 301, station 302 recorded more events later in the deployment. The apparent diurnal signal in the dataset also argues against instrument settling as a likely cause for these events. Finally, the OBSs on the flanks of the volcano would be expected to record similar signals if they were a result of settling.

The impulsive onset and smoothly decreasing coda of type 1 events resemble signals generated by OBSs struck by biological organisms (Buskirk *et al*. 1981). A series of transient pull tests performed on OBSs lying in soft sediment also produced very similar signals due to resonance caused by poor coupling (Tréhu 1985). Thus, type 1 events are very consistent with the signals expected from biological organisms striking the instrument.

Type 2 events are more difficult to explain in terms of biological processes. The low-amplitude initial arrival and high amplitude second arrival could be the result of an organism landing on and then taking off from the instrument. In that case, the first motions of the two arrivals should be consistently reversed. However, this was not observed. Type 2 events may be arrivals from an impulsive source located some distance from the instrument, as the waveforms resemble signals generated by explosive charges in soft sediment (Tréhu 1985).

Type 2 and 3 events might be LP seismicity occurring beneath the sea floor. Type 3 events have similar durations and seismograms as to LP events detected on land during a seismic array study at Deception Island (Alguacil *et al*. 1999) although the land events had a peak frequency of 1–3 Hz, which is lower than the peak frequency of type 3 events. A study investigating rhythmic LP events on Deception Island found that ocean noise was triggering seismicity near the inner shore of Port Foster (Stich *et al*.

https://doi.org/10.1017/S0954102013000758 Published online by Cambridge University Press

2011). Several of the LP seismograms presented in their study resemble type 2 events in both duration and waveform characteristics, although the LP peak frequency is less than half the Port Foster event peak frequency (*c*. 2 Hz as opposed to 4–6 Hz). A histogram of LP activity per day (Stich *et al*. 2011) shows similar clustering and event frequency as Port Foster events although the Port Foster events are not uniformly spaced. Stich *et al.* did not indicate whether there was diurnal or semidiurnal periodicity in these events.

The increased rate of type 3 events at night as opposed to the decrease at night observed for types 1 and 2 events (Table I) might be taken as evidence that the type 3 events have a distinct source. However, the histograms of event counts in 8-hour intervals (Fig. 3) show that the three types of Port Foster event have similar patterns of occurrence, particularly on stations 213 and 301, which suggests a similar source process. Therefore, it is unlikely that some are due to biological activity and others to geological activity. If biological organisms are causing the signals, then the more complex arrivals in type 3 events might result from a creature crawling or brushing over the OBS. However, the consistent signal of the type 2 events is harder to explain unless the creature first hits the sea floor and then the sensor. An earlier study found that biological events are dependent on the diurnal cycle to a depth of 1000 m (Buskirk *et al*. 1981). Since there is an apparent relationship between event frequency and time of day (Fig. 6 and Table I), a biological source is perhaps most likely. Since we see no evidence for similar events on OBSs at similar depths outside Port Foster, any biological cause must be concentrated in the caldera. However, a diurnal signal might be difficult to discriminate from a tidal signal in such a short dataset, particularly in light of the 25-hour periodicity observed in the autocorrelation for station 302 (Fig. 7a). Furthermore, quasi-diurnal volcanic seismicity has been observed on land at Merapi volcano (Fadeli *et al*. 1991), indicating that diurnality alone cannot prove a biological source.

Port Foster events could originate from volcanic or hydrothermal activity, perhaps due to gases or fluids bubbling up from the sea floor. Gas and fluid related signals are common throughout the world. For example, an OBS network deployed in the Sea of Marmara recorded thousands of events that resemble type 1 and type 3 Port Foster events (Tary *et al*. 2012). Some of these events produced strong horizontal particle motions, and all of them attenuated extremely rapidly in the soft substrate on the sea floor. The events were strongly clustered in time, ranging from less than ten per day to over 270 in one day during a swarm, but showed no diurnal or tidal signal. Some events could be correlated between a pair of OBSs located 10 m apart, but instruments located further apart did not detect common events. Tary *et al*. (2012) attribute these events to gas bubbles rising through conduits in the sea floor. They note that geophysical and visual evidence of active degassing has been found in the Sea of Marmara, and that the OBS with the most recorded events was located near a gas-rich fault. Tides in the Sea of Marmara are minimal, perhaps accounting for the lack of tidal periodicity in the event distribution.

Similar signals have been detected in the Galicia Bank of western Spain. These signals consisted of short impulsive events as well as tremor and showed a semidiurnal periodicity attributed to tides. The impulsive events resemble type 1 Port Foster events. The wide variety of amplitudes along with the detection of multiple classes of events led the authors to reject a biological explanation in favour of resonating fluid-filled cracks (Díaz *et al*. 2007).

Sohn *et al*. (1995) observed thousands of events resembling type 1 and type 3 Port Foster events on a hydrothermally active region on the cleft segment of the Juan de Fuca mid-ocean ridge. The OBSs were approximately 4 km apart and none of these events were recorded on multiple instruments. Like signals in the Sea of Marmara and on the Galicia Bank, the events tended to be clustered. The investigators note that the source of these signals cannot be unambiguously determined, but they found that both rock fracturing and vibrating fluids could explain the signals.

The three studies discussed above each describe signals similar to those recorded at Deception Island, and each study takes place in a different tectonic setting. Therefore, it is possible that Port Foster events represent a type of rapidly attenuating geologic signal, perhaps from volcanic gases escaping from the sea floor or hydrothermal fluids resonating in cracks. Fumaroles and hydrothermal activity occur in numerous places along the inner shoreline of the caldera (Ibáñez *et al*. 2000) and likely extend onto the sea floor (Ortiz *et al*. 1992). The apparent diurnal signal that we attribute to the day/night cycle might also result from a 25-hour tidal cycle (Fig. 7). The ocean tides at Deception Island have a semidiurnal amplitude of 1.32 m and diurnal amplitude of 1.14 m (Vidal *et al*. 2012). However, we see no evidence for a significant semidiurnal signal in the correlogram.

Particle motions of the three types of Port Foster events did not suggest the presence of different seismic phases in each signal, although seismograms of type 2 events show two distinct arrivals. The general uniformity of particle motions may be a result of rocking resonances caused by poor coupling masking the true ground motion (Tréhu 1985). Particle motions in the horizontal plane do not show a consistent orientation, suggesting that signals are arriving from all directions and are not compatible with a rocking resonance in one direction. The strong horizontal motions may be due to either poor coupling on the sea floor (Duennebier & Sutton 2007) or a source producing little vertical displacement (Tary *et al*. 2012), or both.

Another possibility is that Port Foster events are very small VT earthquakes occurring very close to the sensor. If the P and S wave arrivals occur almost simultaneously,

https://doi.org/10.1017/S0954102013000758 Published online by Cambridge University Press

it would be very difficult to distinguish an earthquake from a direct perturbation of the instrument. For example, given a P velocity of 3 km second^{-1} for the upper 2 km of material in Port Foster (Zandomeneghi *et al*. 2009), and assuming the substrate is a Poisson solid, an earthquake occurring 127 m from the instrument would have a P to S separation of 0.1 seconds. Since this separation is not observed, the seismic source would have to be even closer. However, the floor of Port Foster is thought to be unconsolidated sediment down to at least 1 km (Zandomeneghi *et al*. 2009), and this substrate is unlikely to experience brittle failure to an appreciable degree. Thus, Port Foster events are probably not small VT earthquakes.

There are an order of magnitude more events recorded at station 213 compared to stations 301 and 302. It is interesting to note that station 213 lies atop an area of uplift attributed to magmatic injection or volcanic resurgence (Cooper *et al*. 1998). Furthermore, the presence of anomalously warm waters in Port Foster (Ortiz *et al*. 1992) implies that hydrothermal activity may be occurring on the sea floor in this region. The presence of events only in Port Foster as well as their concentration near station 213 could be explained by a hydrothermal or volcanic source, or alternatively by a biological organism whose activity is dependent on hydrothermal output.

Future researchers must carefully consider how they will distinguish between objects striking the OBS versus events with rapidly attenuating signals. Perhaps the best way to do this is to bury the OBS, isolating the detector from organisms in the water column while improving coupling with the surrounding sediment (Duennebier & Sutton 2007). However, such operations are costly, may be impractical in remote areas and will not protect against burrowing organisms. OBSs with high-frequency hydrophones could provide a means to discriminate between volcanic/hydrothermal and biological events, since signals caused by collisions should not be observed simultaneously on the seismometer and the hydrophone. However, Tary *et al*. (2012) note that their events were not detected by hydrophones except when the hydrophones were located within 30 cm of the sea floor. Another practical method is to deploy two OBSs side by side to see if the signals appear on both of them (Tary *et al*. 2012), or to include an underwater camera to directly observe the environment around the instrument.

Conclusion

Volcanic seismicity was low at Deception Island during the 2005 field season but OBSs deployed in the flooded caldera of the volcano recorded thousands of events. These events might be attributed to biological activity or volcanic activity. The presence of an apparent diurnal pattern in the rate of events suggests that a biological source is more likely. However, the events are very similar to signals caused by subsurface fluid flow and gas bubbles on the sea floor. Identifying the source model for very localized signals recorded on OBSs remains a challenging problem. Future OBS deployments in Port Foster, and elsewhere, must have a robust strategy for distinguishing between objects striking the instrument and seismic waves passing through the sea floor.

Acknowledgements

This research would not have been possible without funding for the TOMODEC experiment provided by the Spanish Institute of Science and Technology grant REN 200-3833 and the US National Science Foundation grants ANT-0230094 and DGE-1144081. We thank Jesus Ibáñez for leading the experiment and Jonathan Lees, Andrew Barclay, Allan Sauter, Anne Tréhu and Spahr Webb for helpful discussions. We would also like to acknowledge Karl Wirth and John Craddock at Macalester College and Matthew Barvenik of GZA GeoEnvironmental for their support and insight during the research process. This paper greatly benefited from reviews by Fred Duennebier, Daria Zandomeneghi, Maya Tolstoy and Anne Tréhu.

References

Alguacil, G., Almendros, J.C., Del Pezzo, E., Garcia, A., Ibáñez, J.M., La Rocca, M., Morales, J. & Ortiz, R. 1999. Observations of volcanic earthquakes and tremor at Deception Island - Antarctica. *Annali Di Geofisica*, **42**, 417–436.

Barclay, A.H., Wilcock, W.S.D. & Ibáñez, J.M. 2009. Bathymetric constraints on the tectonic and volcanic influences at Deception Island volcano, South Shetland Islands. *Antarctic Science*, **21**, 153–167.

Barker, D.H.N. & Austin, J.A. 1998. Rift propagation, detachment faulting, and associated magmatism in Bransfield Strait, Antarctic Peninsula. *Journal of Geophysical Research - Solid Earth*, **103**, 24 017–24 043.

Ben-Zvi, T., Wilcock, W.S.D., Barclay, A.H., Zandomeneghi, D., Ibáñez, J.M. & Almendros, J. 2009. The P-wave velocity structure of Deception Island, Antarctica, from two-dimensional seismic tomography. *Journal of Volcanology and Geothermal Research*, **180**, 67–80.

Buskirk, R.E., Frohlich, C., Latham, G.V., Chen, A.T. & Lawton, J. 1981. Evidence that biological-activity affects ocean bottom seismograph recordings. *Marine Geophysical Researches*, **5**, 189–205.

Chouet, B. 1996. Long-period volcano seismicity: its source and use in eruption forecasting. *Nature*, **380**, 309–316.

Cooper, A.P.R., Smellie, J.L. & Maylin, J. 1998. Evidence for shallowing and uplift from bathymetric records of Deception Island, Antarctica. *Antarctic Science*, **10**, 455–461.

Díaz, J., Gallart, J. & Gaspà, O. 2007. Atypical seismic signals at the Galicia Margin, north Atlantic Ocean, related to the resonance of subsurface fluid-filled cracks. *Tectonophysics*, **433**, 1–13.

Duennebier, F.K. & Sutton, G.H. 2007. Why bury ocean bottom seismometers? *Geochemistry, Geophysics, Geosystems*, **8**, 1–13.

Fadeli, A., Rydelek, P.A., Emter, D. & Zürn, W. 1991. On volcanic shocks at Merapi and tidal triggering. *In* Schick, R. & Mugiono, R., *eds. Volcanic tremor and magma flow*. Jülich: Forschungszentrum Jülich GmbH, 165–182.

Gasparini, P., Scarpa, R. & Aki, K. 1992. *Volcanic seismology*. New York: Springer, 572 pp.

Ibáñez, J.M., Almendros, J., Carmona, E., Martínez-Arévalo, C. & Abril, M. 2003a. The recent seismo-volcanic activity at Deception Island volcano. *Deep Sea Research II - Topical Studies in Oceanography*, **50**, 1611–1629.

Ibáñez, J.M., Carmona, E., Almendros, J., Saćcorotti, G., Del Pezzo, E., Abril, M. & Ortiz, R. 2003b. The 1998–1999 seismic series at Deception Island volcano, Antarctica. *Journal of Volcanology and Geothermal Research*, **128**, 65–88.

Ibáñez, J.M., Del Pezzo, E., Almendros, J., La Rocca, M., Alguacil, G., Ortiz, R. & García, A. 2000. Seismovolcanic signals at Deception Island volcano, Antarctica: wave field analysis and source modeling. *Journal of Geophysical Research - Solid Earth*, **105**, 13 905–13 931.

Lindquist, K. & Quinlan, D. 2009. *Antelope 4.11 reference guide*. Boulder, CO: BRTT Inc, 53 pp.

Ortiz, R., Vila, J., Garcia, A., Camacho, A.G., Diez, J.L., Aparicio, A., Soto, R., Viramonte, J.G., Risso, C., Menegatti, N. & Petrinovic, I. 1992. Geophysical features of Deception Island. *In* Yoshida, Y., Kaminuma, K. & Shiraishi, K., *eds*. *Recent progress in Antarctic earth science. Proceedings of the Sixth International Symposium on Antarctic Earth Sciences*. Tokyo: Terra Scientific Publishing Company (TERRAPUB), 443–448.

R CORE TEAM. 2012. *R: a language and environment for statistical computing*. Vienna: R Foundation for Statistical Computing, 3349 pp.

Rey, J., Somoza, L. & Martínez-Frías, J. 1995. Tectonic, volcanic, and hydrothermal event sequence on Deception Island (Antarctica). *Geo-Marine Letters*, **15**, 1–8.

Rydelek, P.A., Sacks, I.S. & Scarpa, R. 1992. On tidal triggering of earthquakes at Campi Flegrei, Italy. *Geophysical Journal International*, **109**, 125–137.

Smellie, J.L. 2001. Lithostratigraphy and volcanic evolution of Deception Island, South Shetland Islands. *Antarctic Science*, **13**, 188–209.

Sohn, R.A., Hildebrand, J.A., Webb, S.C. & Fox, C.G. 1995. Hydrothermal microseismicity at the megaplume site on the southern Juan de Fuca ridge. *Bulletin of the Seismological Society of America*, **85**, 775–786.

Sterne, T.E. 1954. Some remarks on confidence or fiducial limits. *Biometrika*, **41**, 275–278.

Stich, D., Almendros, J., Jiménez, V., Mancilla, F. & Carmona, E. 2011. Ocean noise triggering of rhythmic long period events at Deception Island volcano. *Geophysical Research Letters*, **38**, 10.1029/2011GL049671.

Tary, J.B., Géli, L., Guennou, C., Henry, P., Sultan, N., çağatay, N. & Vidal, V. 2012. Microevents produced by gas migration and expulsion at the seabed: a study based on sea bottom recordings from the Sea of Marmara. *Geophysical Journal International*, **190**, 993–1007.

Tréhu, A.M. 1985. Coupling of ocean bottom seismometers to sediment: results of tests with the United States Geological Survey ocean bottom seismometer. *Bulletin of the Seismological Society of America*, **75**, 271–289.

Vidal, J., Berrocoso, M. & Fernández-Ros, A. 2012. Study of tides and sea levels at Deception and Livingston islands, Antarctica. *Antarctic Science*, **24**, 193–201.

Vila, J., Ortiz, R., Correig, A.M. & García, A. 1992. Seismic activity on Deception Island. *In* Yoshida, Y., Kaminuma, K. & Shiraishi, K., *eds*. *Recent progress in Antarctic earth science. Proceedings of the Sixth International Symposium on Antarctic Earth Sciences*. Tokyo: Terra Scientific Publishing Company (TERRAPUB), 449–456.

Zandomeneghi, D., Barclay, A., Almendros, J., Ibáñez Godoy, J.M., Wilcock, W.S.D. & Ben-Zvi, T. 2009. Crustal structure of Deception Island volcano from P-wave seismic tomography: tectonic and volcanic implications. *Journal of Geophysical Research - Solid Earth*, **114**, 10.1029/2008JB006119.